
Article:
Bai, L orcid.org/0000-0001-9016-1569, Zhang, L, Lin, G et al. (1 more author) (2016) Pool boiling with high heat flux enabled by a porous artery structure. Applied Physics Letters, 108 (23). ISSN 0003-6951

https://doi.org/10.1063/1.4953574

Pool boiling with high heat flux enabled by a porous artery structure

Lizhan Bai,[1, 2, *] Lianpei Zhang,[1] Guiping Lin,[1] and G.P. Peterson[3]

[1]Laboratory of Fundamental Science on Ergonomics and Environmental Control, School of Aeronautic Science and Engineering, Beihang University, Beijing 100191, PR China

[2]School of Chemical and Process Engineering, University of Leeds, Leeds, LS2 9JT, UK

[3]George W. Woodruff School of Mechanical Engineering, Georgia Institute of Technology, Atlanta, Georgia 30332, USA

A porous artery structure utilizing the concept of "phase separation and modulation" is proposed to enhance the critical heat flux of pool boiling. A series of experiments were conducted on a range of test articles in which multiple rectangular arteries were machined directly into the top surface of a 10.0 mm diameter copper rod. The arteries were then covered by a 2.0 mm thickness microporous copper plate through silver brazing. The pool wall was fabricated from transparent Pyrex glass to allow a visualization study, and water was used as the working fluid. Experimental results confirmed that the porous artery structure provided individual flow paths for the liquid supply and vapor venting, and avoided the detrimental effects of the liquid/vapor counter flow. As a result, a maximum heat flux of 610 W/cm^2 over a heating area of 0.78 cm^2 was achieved with no indication of dryout, prior to reaching the heater design temperature limit. Following the experimental tests, the mechanisms responsible for the boiling CHF and performance enhancement of the porous artery structure were analyzed.

As one of the most efficient heat transfer modes, nucleate boiling, provides very high heat fluxes, with a relatively small superheat on the heated surface. As a result of this excellent heat transfer performance, nucleate boiling has been applied in a wide variety of areas, including the thermal management of advanced high power electronics, cooling of the nuclear power reactors, thermosyphon heat exchangers and spacecraft thermal control. [1-3] However, the critical heat flux (CHF) limitation, beyond which the temperature of the heated surface will rise sharply with a corresponding significant decrease in the surface heat flux. As the heat flux increases for

* Author to whom correspondence should be addressed.
Electronic mail: bailizhan@buaa.edu.cn

nucleate boiling on a flat surface, more and more bubbles are generated. These bubbles begin to coalesce to form a stable vapor blanket, which prevents the liquid replenishment of the heated surface. Because the thermal conductivity of the vapor is very low, the vapor blanket forms a thermal barrier between the heated surface and the liquid/vapor interface, resulting in the so-called "heat transfer crisis". In real engineering applications, once the surface heat flux exceeds the CHF, the failure of nucleate boiling will lead to rapid burnout of the devices to be cooled. For this reason, it is essential to enhance the CHF of nucleate boiling in order to further expand the range of application areas and guarantee safe and continuous operation.

In general, an entire nucleate boiling consists primarily of three processes: liquid replenishment to the heated surface, vapor venting from the heated surface and efficient heat transfer from the heated surface to the liquid/vapor interface. These three processes are not independent, and there is strong mutual interaction among them. Once any one single process is interrupted, the other two will also be affected, resulting in ultimate failure of the nucleate boiling process. Any method used to enhance the CHF of nucleate boiling should therefore, necessarily focus on the improvement of one or more of these three processes.

The passive measures previously utilized to enhance the CHF of nucleate boiling can be generally categorized into two types: First is through changes in the thermophysical properties of the boiling fluid, such as the addition of different surfactants or the employment of different nanofluids;[4-7] and second is through modifications to the heated surface. In this latter case, a variety of methods have been proposed, such as the fabrication of nano- or micro-scale functional structures,[8-12] deposited nanoparticle layers,[13-18] atomic layer deposition,[19-20] micro/nano porous coatings[21-25] and hybrid wettability treatments.[26-28] Significant progress has been made in the area of CHF enhancement. In particular, the CHF of nucleate boiling for a

smooth surface was enhanced by a factor of three through the use of a modulated microporous coating applied directly onto the heated surface.[29]

In order to further increase the CHF, the current investigation explores the use of a porous artery structure based on the concept of "phase separation and modulation". The porous artery structure can actively formulate the flow paths for liquid replenishment and vapor venting, while helping to maintain the liquid/vapor interface in the porous structure, immediately adjacent to the heated surface. Experimental studies are performed to validate this concept, and are reported in detail below.

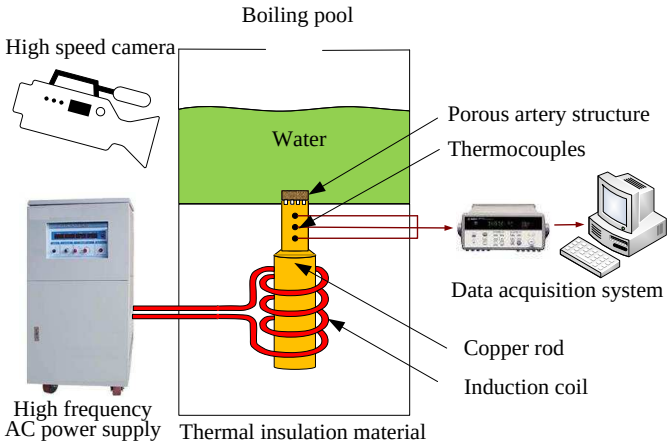

FIG. 1. Schematic of the experimental system

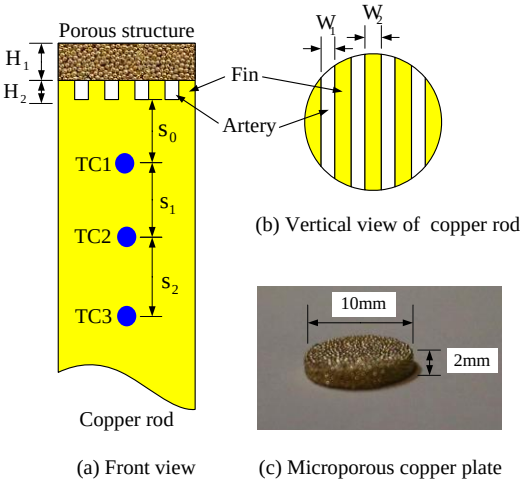

FIG. 2. Schematic of the porous artery structure

Figure 1 illustrates the experimental test facility utilized in the current investigation, which was comprised of a visulization system, a boiling pool, a porous artery structure, the heat source and the temperature measurement and data acquisition system. Figure 2 illustrates a schematic of the porous artery structure and the temperature measurement locations. As shown in Fig. 2, multiple rectangular arteries were machined directly into the top surface of a small copper rod with a diameter of 10.0 mm. These were then covered by a microporous copper plate with a

thickness of 2.0 mm by silver brazing, to form the porous artery structure. Table 1 presents the basic parameters of the porous artery structure.

TABLE 1. Basic parameters of the porous artery structure

Item	Parameters
Porous plate thickness(H_1)/mm	2.0
Porous plate pore size range/mm	0.25-0.38
Artery width(W_1)/mm	1.0
Artery depth(H_2)/mm	1.5
Fin width(W_2)/mm	1.2
Distance s_0, s_1, s_2/mm	10.0, 10.0, 10.0

The boiling pool had an inner diameter of 15 cm and a height of 15cm and was directly open to the ambient atmosphere, so the boiling fluid, i.e. deionized water, was always subject to the atmospheric pressure. The wall of the boiling pool was made of transparent Pyrex glass to provide an opportunity for the visualization study, and the bottom of the boiling pool was made of stainless steel with a thickness of 1.0 mm. A through hole was located at the center of the bottom plate with an inner diameter of 12 mm, so that the small copper rod could pass through it to heat the water directly. The gap between the copper rod and the stainless steel plate was filled with silicone grease to provide a positive seal and also a good thermal insulation between the copper rod and the plate. An electromagnetic induction heater served as the heat source, which could be adjusted continuously by altering the AC power input over the range of 0-10 kW. A maximum heat flux of ~ 600 W/cm^2 could be achieved on the top surface of the small copper rod, limited only by the melting temperature of copper.

High temperature thermal insulation materials were used to insulate the electromagnetic induction heater, in order to reduce the heat loss to the ambient suroundings. The temperature measurement and data acquisition system was composed of several type K thermocouples and an Agilent 34970A Data Acquisition System linked to a PC for data display and storage. Three

thermocouples were firmly attached on the side surface of the small copper rod at a distance of 10 mm, as shown in Fig. 2 (a).

Through the temperature data obtained from the thermocouples, the heat flux (q), superheat (ΔT) and evaporation/boiling heat transfer coefficient (h) can be calculated as follows:

$$q = \frac{k(T_{\mathrm{TC3}} - T_{\mathrm{TC1}})}{s_1 + s_2} \tag{1}$$

$$\Delta T = T_{\mathrm{w}} - T_{\mathrm{s}} = T_{\mathrm{TC1}} - \frac{q s_0}{k} - T_{\mathrm{s}} \tag{2}$$

$$h = \frac{q}{\Delta T} \tag{3}$$

where T_s is the saturation temperature of the working fluid, T_w is the wall temperature, and k is the thermal conductivity of copper.

A comprehensive uncertainty analysis was conducted, using a standard approach as follows:

$$\sigma_q = \sqrt{2\left(\frac{k}{s_1 + s_2}\right)^2 \sigma_{\mathrm{T}}^2 + \frac{\mathrm{k}^2 (T_{\mathrm{TC3}} - T_{\mathrm{TC1}})^2}{(s_1 + s_2)^4} \sigma_{\mathrm{s}}^2} \tag{4}$$

$$\sigma_{\Delta T} = \sqrt{\sigma_{\mathrm{T}}^2 + \frac{q^2}{\mathrm{k}^2} \sigma_{\mathrm{s}}^2 + \frac{s_0^2}{\mathrm{k}^2} \sigma_{\mathrm{q}}^2} \tag{5}$$

$$\sigma_h = \sqrt{\frac{q^2}{(\Delta T)^4} \sigma_{\Delta T}^2 + \frac{\sigma_{\mathrm{q}}^2}{(\Delta T)^2}} \tag{6}$$

The uncertainty of the temperature measurement as determined by the thermocouples, σ_T, was approximately ± 0.5 ℃, and the uncertainty of the distance between two adjacent thermocouple locations, σ_s, was determined to be ± 0.20 mm. Using these values and equation (4), for a heat flux greater than 100 W/cm^2, the relative uncertainty is less than 1.80%.

In the experiment, the criterion for judgement of the CHF is a sudden continuous temperature rise of the heated surface. Meanwhile, the heated surface is completely covered by a vapor layer through visual observation. The experimental test facility was calibrated, first by measuring the pool boiling characteristics on a 10.0 mm diameter, smooth copper surface. The experimental

results were then compared with both the experimental and analytical data available in the literature. Figure 3 and Table 2 present a comparison of the data obtained using the current facility and those reported from other investigations. As illustrated in Fig. 3 and Table 2, the data obtained in the current study are very close to the experimental results of Li, et al. and the theoretical results of Moissis and Berenson, but are slightly higher than the results from the other investigators. This variation may be the result of the relative roughness of the heating surface, coupled with the small size of the heater, i.e., 10.0 mm in diameter, which is much smaller than the Taylor wavelength of 15.7 mm for water at 100 °C. The results of the current investigation, however, exhibit good repeatability, indicating that it can be used to provide high quality and repeatable results in the study of the boiling characteristics of the porous artery structure.

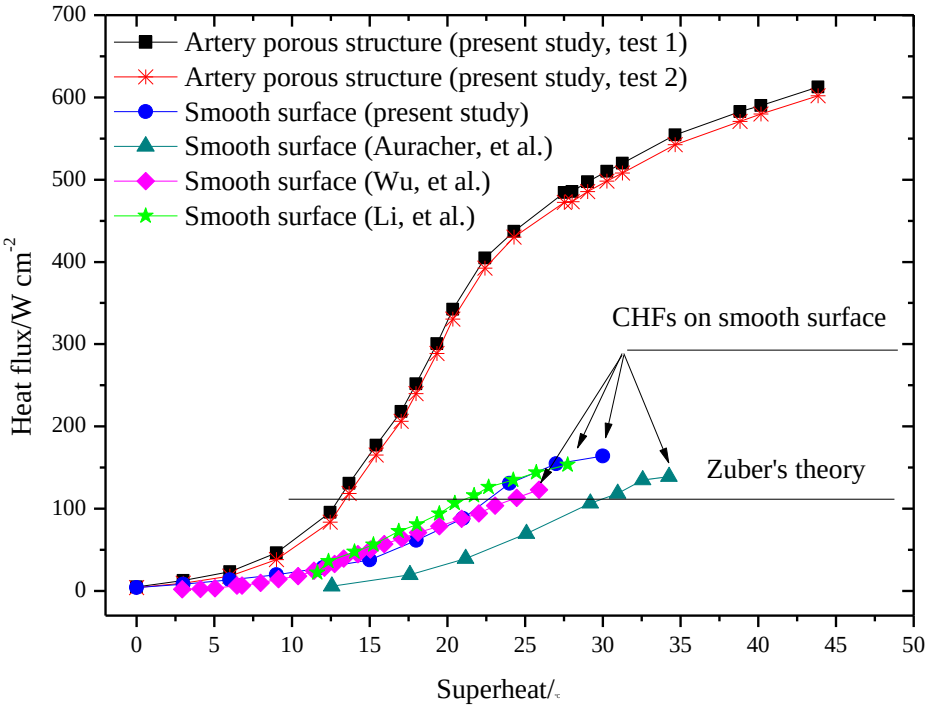

FIG. 3. Superheat dependence of heat flux for smooth surface and porous artery strucure

Figure 3 illustrates the superheat dependence of the heat flux for the porous artery strucure. As shown in Fig. 3, for boiling in the porous artery structure, the heat flux initially increases slowly with the increase of the superheat. Once the superheat exceeds approximately 10 ℃, the heat flux

begins to increase more quickly until it reaches about 400 W/cm^2, then it begins to increase relatively slowly until the attainment of 610 W/cm^2. It is clear that for the boiling in the porous artery structure, no real CHF was observed in the experiments, and the maximum heat flux of 610 W/cm^2 is still far smaller than the actual CHF. A better heater design that can sustain higher temperatures should be considered to achieve even higher heat flux in further studies. To summarize, two important conclusions can be obtained from Fig. 3: First, the use of the porous artery strucutre, allows very high levels of heat flux to be achieved, i.e., 610 W/cm^2, which in the current investigation was limited by the maximum heater design temperature; second, the boiling heat transfer performance is much better than that previously observed for a smooth surface, especially when the heat flux for the porous artery structure is greater than 100 W/cm^2.

TABLE 2. Comparison of CHF of water boiling on a smooth copper surface

Authors	CHF	Heated surface area
Zuber (Model)[30]	110.8 W/cm^2	N/A
Moissis and Berenson (Model)[30]	152.4 W/cm^2	N/A
Lienhard and Dhir (Model)[30]	126.9 W/cm^2	N/A
Auracher et al. (Test data)[31]	139.0 W/cm^2	Φ35mm
Chen Li, et al. (Test data)[24]	149.7 W/cm^2	8mm×8mm
Wu, et al. (Test data)[32]	121.0 W/cm^2	10mm×10mm
C.H. Li, et al. (Test data)[29]	141.3 W/cm^2	8mm×8mm
Present study (Test data)	156.8 W/cm^2	Φ10mm

Figure 4 illustrates the liquid/vapor distribution and bubble movement in the porous artery structure at different superheat values as observed in the experiments. As illustrated in Fig. 4, there is no bubble generation on the top of the porous structure; instead, bubbles always coming out from the arteries at both sides, then flow upwards into the pool. In addition, the larger the superheat, the higher the bubbles can reach at the exit of the arteries. At a very high superheat, i.e., > 30°C, continuous vapor columns appear at the outlets of the arteries. These arteries appear to be unstable and swing violently back and forth as the bubbles rise in the boiling pool.

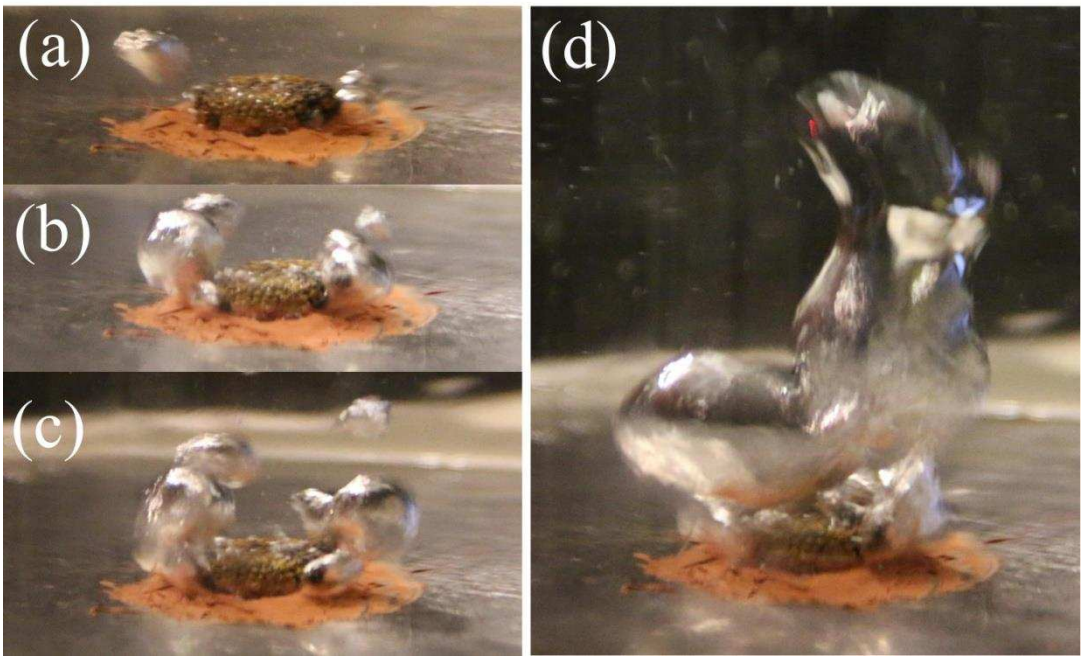

FIG. 4. Liquid/vapor distribution and bubble movement in the porous artery structure at different superheat: (a) △T= 10℃; (b) △T= 20℃; (c) △T= 30℃; (d) △T= 40℃.

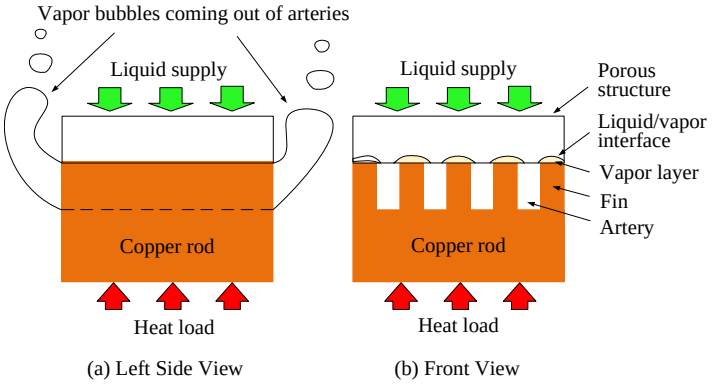

FIG. 5. Schematic of liquid\vapor distribution and bubble movement at high heat fluxes

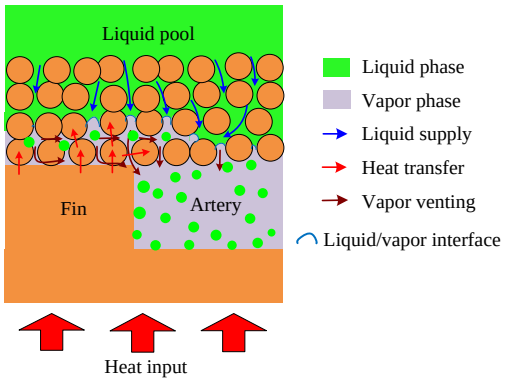

FIG. 6. Schematic of liquid\vapor distribution inside the porous structure at high heat fluxes

Figures 5 and 6 help to illustrate how the porous artery structure can enhance the CHF of pool boiling. It is well known that liquid pumping and vapor blocking are the two basic functions for a porous structure in most two-phase heat transfer applications, where a capillary pressure can be developed at the liquid/vapor interface, as expressed by equation (7):

$$\Delta P_{\text{cap}} = \frac{2\sigma \cos\theta}{r_{\text{e}}} \qquad (7)$$

At high heat fluxes, this capillary pumping helps to continuously replenish liquid directly to the liquid/vapor interface through the porous structure. Due to the capillary pressure developed in the porous structure, vapor generated at the liquid/vapor interface is prevented from flowing upwards directly to the pool, and instead it escapes through the multiple arteries to the pool, as shown in Fig. 5. Consequently the mutual impediments of liquid/vapor counter flow, which is a very severe issue for nucleate boiling on a flat surface, is inhibited and effectively reduced. Meanwhile, compared to film boiling where a vapor blanket separates the heated surface and the liquid/vapor interface, in the porous artery structure investigated here, the liquid/vapor interface is always located in the porous structure very adjacent to the top surface of the fins. Between the heated surface and the liquid/vapor interface is a very thin layer of porous strucutre with a much higher effective thermal conductivity than that of vapor, so the heat transfer from the heated surface to the liquid/vapor interface can always proceed in a very efficient manner, thereby minimizing the causes of boiling crisis. Furthermore, the multiple arteries machined directly into the top surface of the copper rod not only provide flow path for vapor venting, but also increase the surface area of the heater. Both phase separation and enlarged heated surface area contribute to the enhancement of the boiling CHF and heat transfer coefficient.

Note that, it is difficult to evaluate precisely the role of "phase separation and modulation" in pool boiling CHF enhancement without the effect of extended heated surface area, through additional experiments with smooth surface + porous structure and with arteries structure without porous structure, as analyzed below. First, the mechanisms including liquid/vapor movement and phase distribution for pool boiling in the three structures (smooth surface + porous structure, arteries structure without porous structure and porous artery structure) are much different from each other. Second, for pool boiling CHF enhancement, the CHF for the porous artery structure

is far larger than those for the smooth surface + porous structure and for the arteries structure without porous structure, and even the sum of CHFs for the latter two structures.

In addition, another important mechanism, i.e., the entrainment of liquid droplets by the high velocity vapor flow in the arteries, as shown in Fig. 6, also contributes to the highly efficient boiling heat transfer in the porous artery structure. Through an approximate calculation of the highest vapor velocity in the arteries by assuming that the heat flux for all the arteries is uniform, the vapor velocity in the arteries may become very large at high heat fluxes, i.e., > 50 m/s at a heat flux of 600 W/cm^2, and under such a condition, it is easy to cause the entrainment phenomena.

As shown in Fig. 3, the boiling heat transfer performance in the porous artery structure is much better than that on a flat surface especially at high heat fluxes. This is possible only when the liquid/vapor two-phase heat transfer occurs on the walls of the arteries; otherwise the thermal conduction through the fins requires a temperature difference of several tens of degrees at high levels of heat flux. The entrainment of liquid is a common phenomenon in conventional heat pipe operation, which will impede the liquid return from the condenser to the evaporator, and degrade the heat transfer performance of the heat pipe. Whereas in this application, the entrainment effect helps to carry multiple liquid droplets to wet the hot walls of the arteries, which significantly benefits the boiling heat transfer performance of the porous artery structure.

Acknowledgement

This work was supported by the National Natural Science Foundation of China (No. 51306009), Beijing Natural Science Foundation (No. 3144031), and the EU Marie Curie Actions-International Incoming Fellowships (FP7-PEOPLE-2013-IIF-626576).

References

[1]V. P. Carey, Liquid-Vapor Phase-Change Phenomena: An Introduction to the Thermophysics of Vaporization and Condensation Processes in Heat Transfer Equipment, 2nd ed. (Taylor & Francis, London, 2007).

[2]An Zou and Shalabh C. Maroo, Appl. Phys. Lett. 103, 221602 (2013).

[3]J. Buongiorno, L. W. Hu, G. Apostolakis, R. Hannink, T. Lucas, and A. Chupin, Nucl. Eng. Des. 239, 941 (2009).

[4]D. S. Wen and B. X. Wang, Int. J. Heat Mass Transfer 45, 1739 (2002).

[5]D. Wen, Appl. Therm. Eng. 41, 2(2012).

[6]Xiande Fang, Run Wang, Weiwei Chen, Helei Zhang, and Chunxiang Ma, Appl. Therm. Eng. 91, 1003(2015).

[7]Dogan Ciloglu and Abdurrahim Bolukbasi, Appl. Therm. Eng. 84, 45(2015).

[8] S. G. Kandlikar, Appl. Phys. Lett.102, 051611 (2013).

[9]H. S. Ahn, N. Sinha, M. Zhang, D. Banerjee, S. Fang, and R. H. Baughman, ASME Trans. J. Heat Transfer 128, 1335 (2006).

[10]C. Li, Z. Wang, P. I. Wang, Y. Peles, N. Koratkar, and G. P. Peterson, Small 4, 1084 (2008).

[11]R. Chen, M. C. Lu, V. Srinivasan, Z. Wang, H. H. Cho, and A. Majumdar, Nano Lett. 9, 548 (2009).

[12]Z. Yao, Y. W. Lu, and S. G. Kandlikar, Int. J. Therm. Sci. 50, 2084 (2011).

[13]S. M. You, J. H. Kim, and K. H. Kim, Appl. Phys. Lett. 83, 3374 (2003).

[14]S. J. Kim, I. C. Bang, J. Buongiorno, and L. W. Hu, Appl. Phys. Lett. 89, 153107 (2006).

[15]H. D. Kim and M. H. Kim, Appl. Phys. Lett. 91, 014104 (2007).

[16]S. D. Park, S. W. Lee, S. Kang, I. C. Bang, J. H. Kim, H. S. Shin, and D. W. Lee, Appl. Phys. Lett. 97, 023103 (2010).

[17]H. S. Ahn, H. J. Jo, S. H. Kang, and M. H. Kim, Appl. Phys. Lett. 98, 071908 (2011).

[18]C. K. Huang, C. W. Lee, and C. K. Wang, Int. J. Heat Mass Transfer 54, 4895 (2011).

[19] Bo Feng, Keith Weaver, and G. P. Peterson, Appl. Phys. Lett. 100, 053120 (2012).

[20]S. M. George, Chem. Rev. 110, 111 (2010).

[21]Ho Seon Ahn, Hang Jin Jo, Soon Ho Kang, and Moo Hwan Kim, Appl. Phys. Lett. 98, 071908 (2011).

[22]S. G. Liter and M. Kaviany, Int. J. Heat Mass Transfer 44(22), 4287 (2001).

[23]S. Li, R. Furberg, M. S. Toprak, B. Palm, and M. Muhammed, Adv. Funct. Mater. 18, 2215 (2008).

[24]Chen Li, and G. P. Peterson, ASME Trans. J. Heat Transfer 129, 1465 (2006).

[25]Chen Li, and G. P. Peterson, J. THERMOPHYS HEAT TR. 24, 449 (2010).

[26]S. Kim, H. D. Kim, H. Kim, H. S. Ahn, H. Jo, and M. H. Kim, Exp. Therm. Fluid. Sci. 34, 487 (2010).

[27]A. R. Betz, J. Xu, H. Qiu, and D. Attinger, Appl. Phys. Lett. 97, 141909 (2010).

[28]K.-H. Chu, R. Enright, and N. Wang, Appl. Phys. Lett. 100, 241603 (2012).

[29]Calvin H. Li, T. Li, Paul Hodgins, Chad N. Hunter, Andrey A. Voevodin, John G. Jones, and G.P. Peterson, Int. J. Heat Mass Transfer 54, 3146 (2011).

[30]L. S. Tong and Y. S. Taung, Boiling Heat Transfer and Two Phase Flow, 2nd ed. (Taylor & Francis, London, 1997).

[31]H. Auracher, W. Marquardt, M. Buchholz, R. Hohl, T. Luttich, and J. Blum, Therm. Sci. Eng., 9, 29 (2001).

[32]W. Wu, H. Bostanci, L.C. Chow, Y. Hong, M. Su, and J.P. Kizito, Int. J. Heat Mass Transfer 53, 1773 (2010).